

Simulations of Hard Nanoparticle Encapsulation during Polymer Micelle Formation

Thesis

Presented in Partial Fulfillment of the Requirements for the Degree Graduation with
Research Distinction in Biomedical Engineering at The Ohio State University

By

Anne Shim

Undergraduate Program in Biomedical Engineering

The Ohio State University

2015

Thesis Committee:

Lisa Hall, Advisor

Tanya Nocera

Barbara Wyslouzil

Copyright by

Anne Shim

2015

Abstract

Polymer-protected medical nanoparticles have become an area of interest for drug delivery and medical imaging. Protection by polymer micelles allows for the use of drugs that are toxic to the body, insoluble in the blood stream, or cleared by the kidneys prematurely. Additionally, drug nanoparticles can be modified to have fluorescent and magnetic properties, which allow for greater control and ease of imaging. However, the molecular process that controls the formation of these micelles is not yet well understood and creating micelles with a controllable size at a commercial level has not yet been accomplished. Because it is not feasible to observe the aggregation process experimentally, it is most effective to use computer models to observe and make predictions. The objectives of this study are to successfully model the encapsulation of nanoparticles during micelle formation using flash nanoprecipitation and to alter the controllable parameters of the system, such as mixing time and solute and polymer concentrations, to suggest parameters for creating homogenous micelles on a commercial scale. We use dissipative particle dynamics (DPD), a coarse-grained simulation method in which each “bead” in the simulation box represents several monomers or water molecules, to study aggregation behavior of a model systems containing water, amphiphilic block copolymers, and nanoparticles. We have observed the aggregation process and have shown how changing certain parameters (e.g. nanoparticle/polymer ratio) affects the system. Understanding which parameter values cause ideal aggregate

formation can lead to commercial availability of polymer protected medical nanoparticles, which allow for more targeted drug delivery and can be of great importance when traditional delivery methods result in widespread cell death.

Acknowledgments

I would like to thank Dr. Lisa Hall for allowing me to be a part of her research group and for entrusting me with this project. Being a part of her group has allowed me to not only learn from her, but also from the other members of her group, which has been invaluable.

I would also like to thank Dr. Jonathan Brown for all of his instruction throughout my time working on this project. This project would not be possible without his continued guidance and support. Finally, I would like to thank Sayantan Banerjee for the work he did to set up the preliminary systems that this project; this work was partially supported by the National Science Foundation grant CMMI-1344567. This work was supported in part by an allocation in computing time from the Ohio Supercomputer Center and a “Research Scholar Award” from the Undergraduate Research Office.

Vita

June 2007.....Queen of Angels Montessori School, Cincinnati, OH
May 2011Turpin High School, Cincinnati, OH
September 2011 to presentThe Ohio State University, B.S. Biomedical
Engineering (Spanish minor)

Fields of Study

Major Field: Biomedical Engineering

Minor Field: Spanish

Table of Contents

Abstract	3
Acknowledgments.....	5
Vita	6
Fields of Study.....	6
List of Figures	8
Chapter 1: Introduction	9
Chapter 2: Methods	13
Chapter 3: Results and Discussion	18
Chapter 4: Conclusion	29
Chapter 5: References	31
Appendix A: Data	33

List of Figures

Figure 1. Coarse-grained model of a polymer.....	14
Figure 2. Initial state of hard nanoparticle system before equilibration.	16
Figure 3. Type of aggregations over time for an intermediate nanoparticle concentration.	19
Figure 4. Average number of micelles for all systems at 12 microseconds.....	20
Figure 5. Polymer and nanoparticle distribution in various types of aggregations over time for an intermediate nanoparticle concentration.....	21
Figure 6. Percent of free polymer for each system at time 12 microseconds.....	21
Figure 7. Average number of polymers in micelles at time 12 microseconds.....	22
Figure 8. Average number of nanoparticles in nanoparticle-containing micelles for each system at time 12 microseconds.....	23
Figure 9. Final state for N=25, 1/5 Hydrophobic. Approximate number of nanoparticles per 100 polymers is 4 (left), 8 (second), 12 (third), 16 (right). Bottom shows nanoparticles in purple, hydrophobic polymer in pink, hydrophilic polymer in blue. Top is shown with transparent polymers.....	24
Figure 10. Final state with N=50, 1/3 Hydrophobic. Approximate number of nanoparticles per 100 polymers is 4 (left), 8 (second), 12 (third), 16 (right). Bottom	

shows nanoparticles in purple, hydrophobic polymer in pink, hydrophilic polymer in blue. Top is shown with transparent polymers.24

Figure 11. Average extent of micelles for all systems at time 12 microseconds.....26

Figure 12. Radius of gyration of micelles for all systems at time 12 microseconds.....27

Figure 13. Polydispersity of micelles for all systems at time 12 microseconds.....27

Chapter 1: Introduction

Computer simulations of nanoparticle encapsulation during polymer micelle formation can serve as a useful tool in understanding how to homogenize large-scale micelle production. First, this project will study the molecular process behind micelle formation, leading to an understanding of how to successfully scale up the process of micelle formation, which is pertinent to the field of Chemical Engineering. Knowing how micelles are formed on the molecular level will indicate how to combine polymers, solvent, and solutes in a way that optimizes production. Currently, micelle creation is only viable in the laboratory setting and is not feasible on a commercial scale because of the inconsistent size and shape that result from large-scale production (4). The field of Biomedical Engineering has become interested in utilizing polymer-protected nanoparticles for drug delivery and medical imaging. Polymer protection allows the delivery of drugs that are toxic to the human body, insoluble in the bloodstream, or prematurely cleared by the kidneys (4). For example, when chemotherapy drugs are protected by polymers which are targeted to certain receptors, positively charged, or pH responsive, they allow for a more controlled release, which reduces the toxicity to non-tumor cells (10). Using a computer model, in addition to physical experiments, to understand this project is an extremely valuable tool. Primarily, it provides a way to visualize and observe the molecular implications of various polymer interactions, which are impossible to observe in physical experiments (1).

Because of the long time and length scales that need to be described for our systems, we will use simple coarse-grained models, which represent multiple atoms as a single interaction site or bead. There is a plethora of previous research exploring Monte Carlo and mean-field methods for studying equilibrium properties of block copolymers. The problem with these methods is they do not allow intensive, in depth study of nonequilibrium properties (1). Due to this, the simulations for this project will be molecular dynamics simulations, which integrate Newton's 2nd law forward in time given pairwise interaction potentials between atoms or particles (3). More specifically, these will be canonical molecular dynamics simulations, which are used to simulate constant-temperature systems and were created as a more accurate model of how physical experiments are performed (2). When canonical simulations are employed, a "thermostat algorithm" is used to maintain constant temperature. The traditional thermostat used in coarse-grained canonical systems is the Langevin thermostat, which employs stochastic dynamics to maintain temperature. However, the disadvantages of using the Langevin thermostat are that it does not conserve momentum and does not accurately represent hydrodynamics. A more recently proposed method, Dissipative Particle Dynamics (DPD), modified the Langevin and Brownian methods to fix these issues (4). The DPD method uses a more coarse-grained model than typical molecular dynamics models, which includes a soft repulsion for the beads. The DPD method will be used for this project.

The models will primarily be used as a way to understand the molecular process that underlies polymer micelle creation. Though there are several methods of creating micelles, the method studied by this project will be flash nanoprecipitation, whereby an amphipathic block copolymer originates in a neutral solvent and is rapidly mixed with water to stimulate aggregate formation. This project will use tetrahydrofuran (THF) as the neutral solvent, water as the polar solvent, polystyrene (PS) as the hydrophobic polymer, polyethylene glycol (PEG) as the hydrophilic polymer, and hydrophobic hard nanoparticles. The structure of these micelles will have the hydrophobic PS polymers surrounded by the hydrophilic PEG polymers. The nanoparticles are encapsulated inside of the polymers during micelle formation. The nanoparticles are modeled as a sphere of PS-like beads.

Experimentally, several types of nanoparticles are of interest for better control and imaging success. These nanoparticles can have fluorescent and magnetic properties. Fluorescent nanoparticles are of interest because of the ease of ascertaining their movement. Understanding the movement of nanoparticles within the human body is important for understanding methods of drug delivery. On the other hand, magnetic nanoparticles are of interest because they are controllable with the use of magnetic fields (8).

Chapter 2: Methods

The system modeled contained polystyrene-*b*-polyethylene glycol (PS-*b*-PEG) polymers, hard nanoparticles, and tetrahydrofuran (THF) and water as the solvent. To simulate the process of flash nanoprecipitation, the polymers and solutes were originally submerged in THF, which was rapidly changed into water (details below). The system used a coarse-grained model, which groups multiple atoms into a larger coarse-grained unit, or “bead,” as depicted in Figure 1. The pairwise interactions between the beads represent the size and the chemical interactions of the atomistic system and were identical to those of Reference 5. For this system, the characteristic length was $L_{\text{DPD}} = 1 \text{ nm}$ and the characteristic energy was $\epsilon_{\text{DPD}} = 4.114 \times 10^{-21} \text{ J}$. Each bead has the same mass $m_{\text{DPD}} = 200 \text{ Da}$ (the characteristic mass of the simulations). Original systems used polymers that were 25 beads in length, which contained a PS block of 5 beads and a PEG block of 20 beads. These compositions were chosen because they correctly represented the melt density of polystyrene and the radius of gyration for polyethylene glycol in water (6). Neighboring beads were held together with harmonic bonds with an equilibrium length of 0.8 nm and a spring constant of 0.25 N/m. The number density of the system was $\rho = 3.0 \text{ nm}^{-3}$. Solvent beads represented 10 molecules in order to match

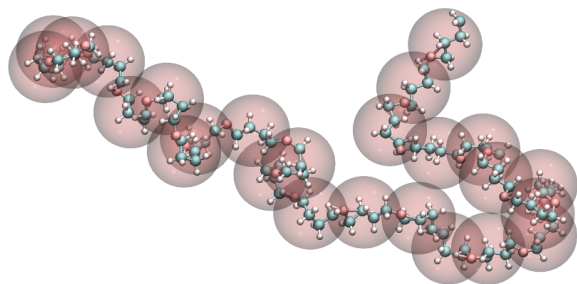


Figure 1: Coarse-grained model of a polymer¹¹

the density of liquid water. To ensure the simulations would match past research and experimental results, this system was run with solutes that were 3 beads in length, which had been used to represent itraconazole, an anti-fungal drug prescribed to cancer patients.

After the original system was successfully modeled, the solutes were replaced with hard nanoparticles. These simulations were designed to reveal how nanoparticles become encapsulated in the polymer during micelle formation. Hard nanoparticles were created by “cutting” a sphere from a DPD simulation of pure solvent in order to create nanoparticles with an amorphous internal structure. (Testing was performed with spheres created using a face-centered cubic lattice of internal beads, but this system was not preferred to model spherical particles since it had small facets due to the crystal structure.) Specifically, beads within a sphere of radius 2 nm at a particular time in the simulation of the fluid of solvent were identified, and all of the beads inside the radius were bonded to nearby particles within a distance of 1.0 nm. There were five bond lengths used: 0.1, 0.3, 0.5, 0.7, or 0.9 nm, depending on the distance between the beads; to assign bond length, the distance between each of the beads was measured and the bond length closest to that distance was fixed as the bond length. The bonded sphere of beads was used as the nanoparticle inserted into the simulations (each nanoparticle in the simulation consists of the same number of beads bonded in the same way as the other nanoparticles, though the bonds are harmonic rather than fixed so exact shape varies very slightly for each over time).

All of the systems studied contained 450 polymers, but the number of nanoparticles in the system varied. The systems contained 18, 35, 53, or 70 nanoparticles, creating four different nanoparticle concentrations, which correspond to approximately 4 nanoparticles per 100 polymers, 8 nanoparticles per 100 polymers, 12 nanoparticles per 100 polymers, and 16 nanoparticles per 100 polymers.

The size and hydrophobicity of polymers were also varied to create four different polymers. These polymers were either 25 beads in length or 50 beads in length. For each length, the size of the PS block was chosen to create polymers that were 1/5 or

approximately 1/3 hydrophobic. For the polymers that were 1/5 hydrophobic and 25 beads in length, the PS block was 5 beads and the PEG block was 20 beads. The polymers that were 1/5 hydrophobic and 50 beads in length had a PS block of 10 beads and a PEG block of 40 beads. The polymers that were approximately 1/3 hydrophobic and 25 beads in length had a PS block of 8 beads and a PEG

block of 17 beads. Finally, the polymers that were approximately 1/3 hydrophobic and 50 beads in length had a PS block of 17 beads and a PEG block of 33 beads. Each of these four polymers was tested with each of the four nanoparticle concentrations, creating sixteen systems in total. The initial state of the systems is shown in Figure 2. This is qualitatively representative of all systems and is the

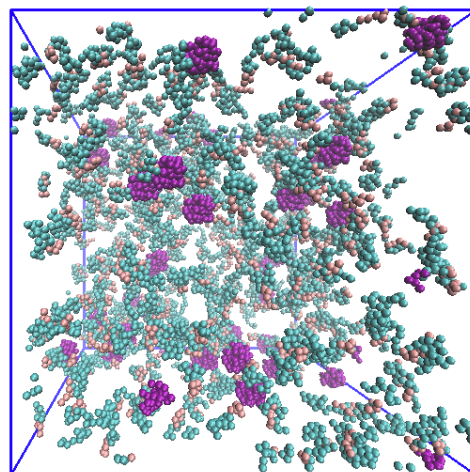


Figure 2: Initial state of hard nanoparticle system before equilibration

initial state of the system with approximately 8 nanoparticles per 100 polymers and polymers that were approximately 1/5 hydrophobic and 25 beads in length.

These simulations were carried out in LAMMPS (Large Scale Atomic-Molecular Massively Parallel Simulator) with the DPD method. DPD represents the force on atom i due to atom j as a sum of three terms $(F^C + F^D + F^R) \vec{r}_{ij}$, where \vec{r}_{ij} is a unit vector pointing from atom j to atom i . F^C is a soft, conservative repulsive force, $F^C = a_{ij} (1 - r/r_c)$, where a_{ij} is the interaction parameter, r is the distance between the beads, and r_c is the diameter of the beads (in our case $r_c = 1 \text{ nm}$ for all interactions). F^D is a dissipative/frictional force, $F^D = -\gamma \left(1 - \frac{r}{r_c}\right)^2 (\vec{r}_{ij} \circ \vec{v}_{ij})$, where γ is the friction coefficient (set to 18.0 for solvent-nonsolvent interactions and 4.5 for all other interactions, corresponding to approximately 2000 ns^{-1} and 500 ns^{-1}) and \vec{v}_{ij} is the vector difference in velocities (bead i minus bead j). Finally, F^R is the random force, $F^R = \sigma \left(1 - \frac{r}{r_c}\right) \alpha (\Delta t)^{-1/2}$, where α is a standard normal random number, Δt is the timestep size, and $\sigma = \sqrt{2k_B T \gamma}$ where k_B is the Boltzmann constant and T is the temperature (11).

The intrinsic timescale one expects based on the initial mapping of bead size and mass to real units is $\tau_{\text{intrinsic,DPD}} = L_{\text{DPD}}(m_{\text{DPD}}/\epsilon_{\text{DPD}})^{0.5} = 9 \text{ ps}$. However, the coarse-graining procedure involves approximations that act to further speed up the dynamics of the system; in order to best map to real experimental timescales, all results were rescaled using $\tau_{\text{DPD}} = 250 \text{ ps}$ as in Reference 5. Each system was run with a timestep of $\Delta t = 0.03 \tau_{\text{DPD}}$, so one can convert to real time using: real ps = (number of time

steps) $\times(0.03\tau_{\text{DPD}}/\text{timestep}) \times(250 \text{ ps}/\tau_{\text{DPD}})$. The repulsion parameter for all like-like interactions was set to $a_{ii} = 25\epsilon_{\text{DPD}}$. The solvent-PS and solvent-NP bead repulsion parameters were also set to $a_{ii} = 25\epsilon_{\text{DPD}}$ for the THF solvent, which changed over the simulation into pure water with a repulsion parameter $a_{ii} = 54\epsilon_{\text{DPD}}$. The PS-PEG and NP bead-PEG repulsion parameter was set to $a_{pe} = 40\epsilon_{\text{DPD}}$.

The simulation run consisted of three parts. The first was a brief equilibration time, which was 100,000 time steps, or 0.75 μs , starting from a random initial configuration (specifically, the particles were placed such that they were not overlapping and solvent and polymers were placed such that they were not inside the particles but otherwise randomly as random walks). During equilibration, the solvent was THF with a solvent-PS and solvent-NP bead repulsion parameter of $a_{ii} = 25\epsilon_{\text{DPD}}$. Next, the THF was changed into water in a stepwise fashion over 800 evenly spaced increments. This phase was the “mixing time” and lasted for 800,000 time steps, or 6 μs . During the mixing time, the solvent-PS and solvent-NP bead repulsion parameters incrementally increased from $a_{ii} = 25\epsilon_{\text{DPD}}$ to of $a_{ii} = 54\epsilon_{\text{DPD}}$. Finally, the system continued to evolve with pure water as the solvent for an additional 800,000 time steps, or 6 μs . During this third period with water solvent, the solvent-PS and solvent-NP bead repulsion parameters were constant at $a_{ii} = 54\epsilon_{\text{DPD}}$. For each system studied, the simulation was run three independent times from three different random initial configurations and the results were averaged together in the data presented below.

Chapter 3: Results and Discussion

For each of the systems, the number of micelles created, the amount of aggregation, and the physical size of micelles created were calculated and compared. Two types of micelles were formed in the systems. The first was aggregations of two or more polymers with a PS interior, protected by a PEG exterior (hereafter referred to as “polymer-only micelles”). The other type of micelle created had a PS and nanoparticle core,

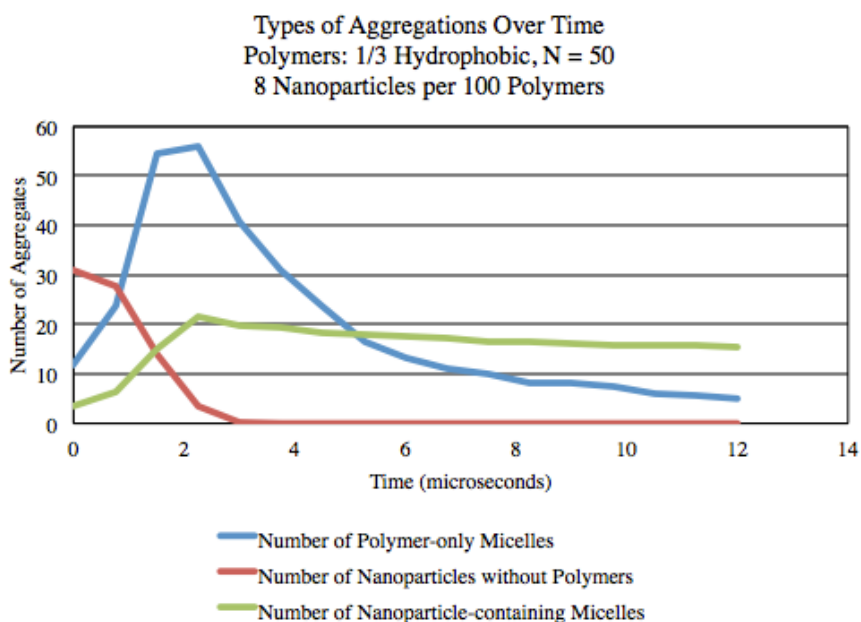


Figure 3: Type of aggregations over time for an intermediate nanoparticle concentration

surrounded by a PEG exterior (hereafter referred to as “nanoparticle-containing micelles”). The trend of the number of these micelles over time was qualitatively the same for all systems, and is shown for an intermediate nanoparticle concentration in

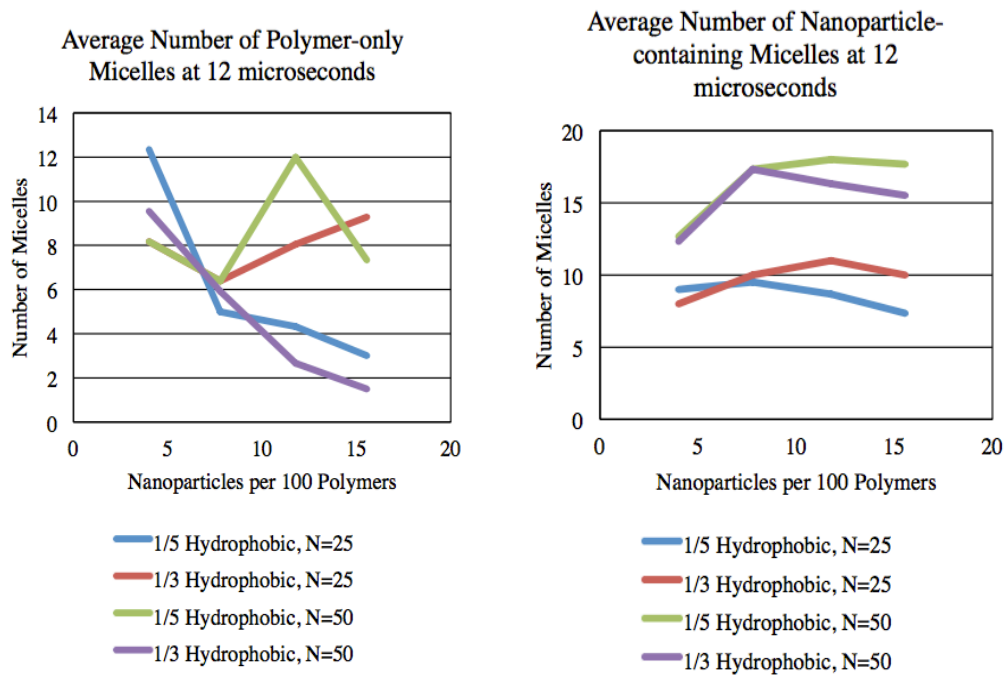


Figure 4: Average number of micelles for all systems at 12 microseconds

Figure 3 (above). All systems finished with a lower number of polymer-only micelles than nanoparticle-containing micelles, which is emphasized by Figure 4, which displays the number of polymer-only micelles and the number of nanoparticle-containing micelles for all systems at the final time (12 microseconds). On average, for all of these systems, there was a greater number of nanoparticle-containing micelles than polymer-only micelles at the end of the simulations. In addition, none of the systems contained nanoparticles that were unprotected by polymers at the final time. For each system, the number of micelles formed over time was calculated and is shown in Figures 14-28 in Appendix A.

To further understand these micelles, the percent of polymer and nanoparticles participating in each micelle type was determined over time.

The results for all systems are shown in Figures 14-28 in Appendix A. All of

these systems consistently showed the same trend, which is displayed in Figure 5 for an intermediate nanoparticle concentration. In all systems, almost all of the polymers and nanoparticles initially began as free polymers (polymers that were not involved in a micelle of any type) and nanoparticles without polymers. However, before the mixing time was over, almost all of the polymers and all of the nanoparticles formed micelles. The only system in which all of the polymers did not form

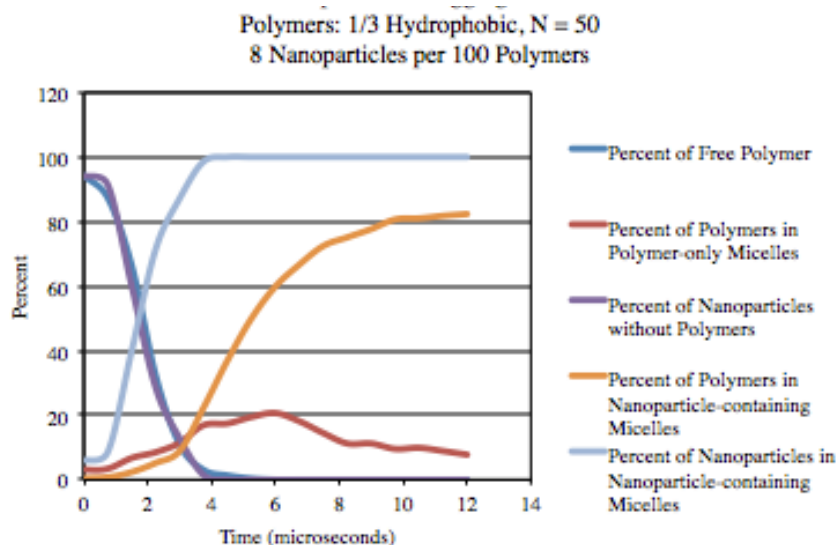


Figure 5: Polymer and nanoparticle distribution in various types of aggregations over time for an intermediate nanoparticle concentration

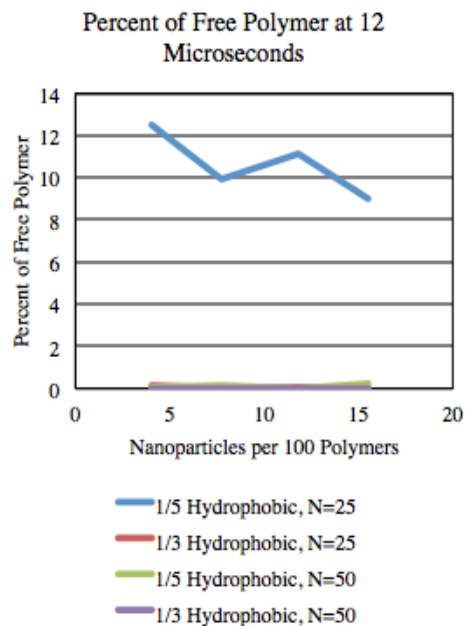


Figure 6: Percent of free polymer for each system at time 12 microseconds

micelles was for the systems with polymers that were 1/5 hydrophobic and had a length of 25 beads. These systems contained free polymers at the end of the simulations, which is emphasized in Figure 6 (above), which displays the percent of free polymer for all systems. This may be because for these smaller polymers with a smaller fraction of hydrophobic monomers, some of the individual polymers can act like small clusters, where the PEG self-protects the PS that it is attached to. This may also be prevalent in the initial equilibrium stage, where the polymers are not held onto the micelles very strongly, allowing them to break off from micelles. As the percent of nanoparticles without polymers decreases, the percent of nanoparticles in nanoparticle-containing micelles increases until all of the nanoparticles are contained in micelles. Additionally, as the

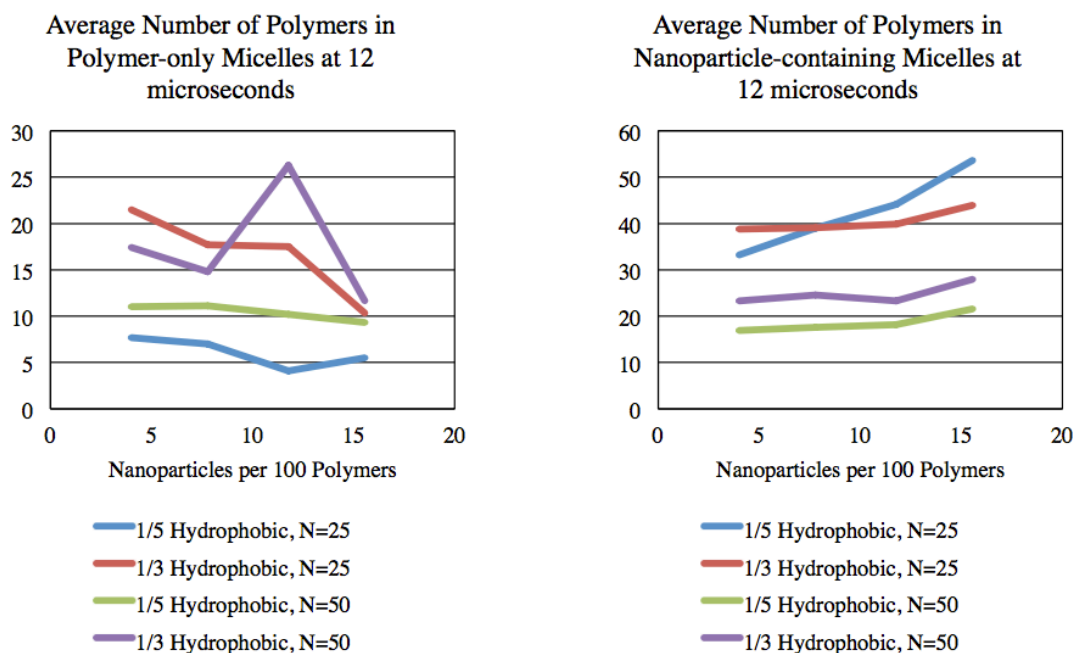


Figure 7: Average number of polymers in micelles at time 12 microseconds

As the percent of nanoparticles without polymers decreases, the percent of nanoparticles in nanoparticle-containing micelles increases until all of the nanoparticles are contained in micelles. Additionally, as the percent of free polymer decreases, the percent of polymer in polymer-only micelles and in nanoparticle-containing micelles increases. However, for all systems, there was a higher percentage of polymers in nanoparticle-containing micelles than in polymer-only micelles. This is emphasized by Figure 7 (above), which displays the number of polymers in polymer-only micelles and the number of polymers in nanoparticle-containing micelles. The systems with polymers of length 25 beads specifically contained a much greater number of polymers in nanoparticle-containing micelles than in polymer-only micelles at the end of the simulation.

The average number of nanoparticles in nanoparticle-containing micelles at the end of the simulation is shown in Figure 8. For these systems, the shorter polymers (N=25) consistently created a larger number of micelles than shorter polymers (N=50). For all systems, there was a lower average number of nanoparticles and polymers per nanoparticle-containing micelle for longer

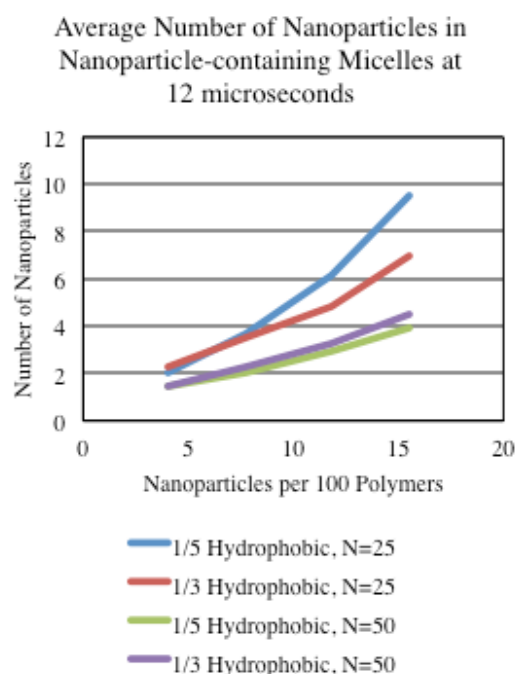


Figure 8: Average number of nanoparticles in nanoparticle-containing micelles for each system at time 12 microseconds

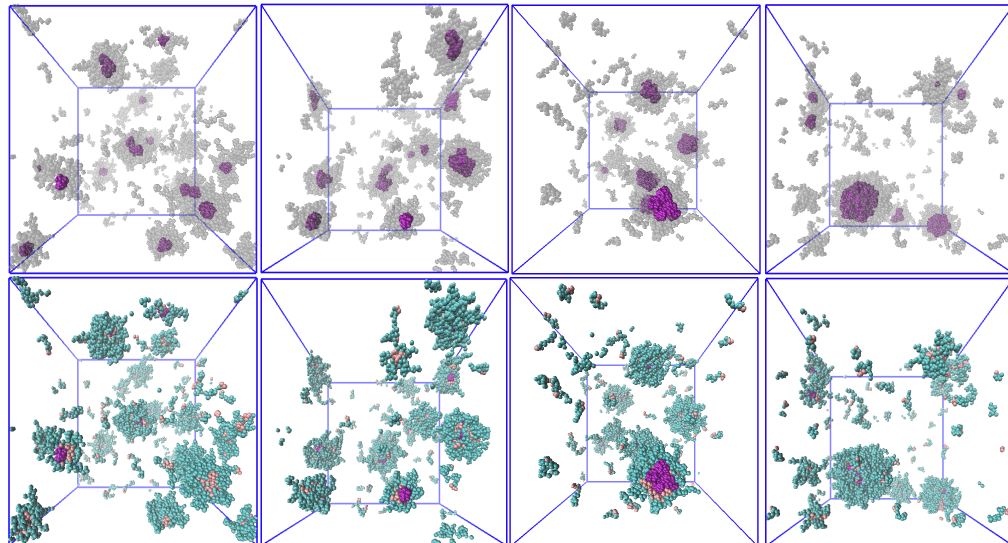


Figure 9: Final state for $N=25$, $1/5$ Hydrophobic. Approximate number of nanoparticles per 100 polymers is 4 (left), 8 (second), 12 (third), 16 (right). Bottom shows nanoparticles in purple, hydrophobic polymer in pink, hydrophilic polymer in blue. Top is shown with transparent polymers

polymers than for shorter polymers. Additionally, for polymers of length 25 beads, less hydrophobic polymers result in a larger average number of nanoparticles and polymers per micelle; however, the reverse is true for polymers of length 50 beads. The final state

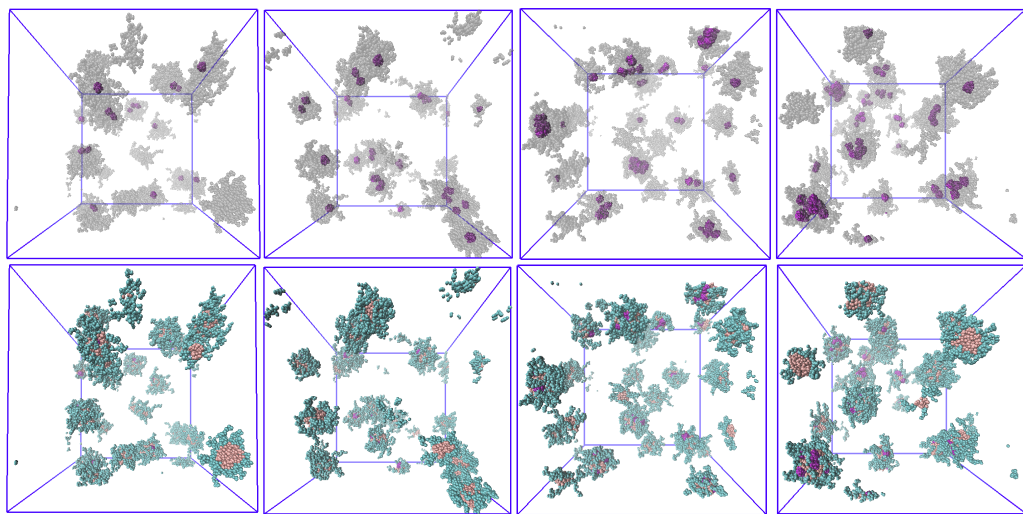


Figure 10: Final state with $N=50$, $1/3$ Hydrophobic. Approximate number of nanoparticles per 100 polymers is 4 (left), 8 (second), 12 (third), 16 (right). Bottom shows nanoparticles in purple, hydrophobic polymer in pink, hydrophilic polymer in blue. Top is shown with transparent polymers

of all systems with polymers that are 1/5 hydrophobic and 25 beads in length is shown in Figure 9 (above) and the final state of all systems with polymers that are 1/3 hydrophobic and 50 beads in length is shown in Figure 10. These figures display the systems with approximately 4 nanoparticles per 100 polymers on the far left, 8 nanoparticles per 100 polymers second, 12 nanoparticles per 100 polymers third, and 16 nanoparticles per 100 polymers on the far right. On the bottom is the final state of the systems and on the top is the system with transparent polymers to better visualize the number of micelles and the number of nanoparticles per micelle in each state. It can be seen in these two figures that the system with free polymer at the end (Figure 9) had a greater dispersity of micelle size than the system with no free polymer at the end. This was explored in more detail by calculating the average radius of gyration and average extent of the micelles at the final time (12 microseconds). The extent is the average difference between the maximum center of mass and the minimum center of mass in the x direction, the y direction, and the z direction. The average extent of polymer-only micelles and nanoparticle-containing micelles is shown in Figure 11 (below). Both of these show that significantly larger micelles were created by the longer polymers ($N=50$). This is echoed by studying the average radius of gyration, shown below in Figure 12.

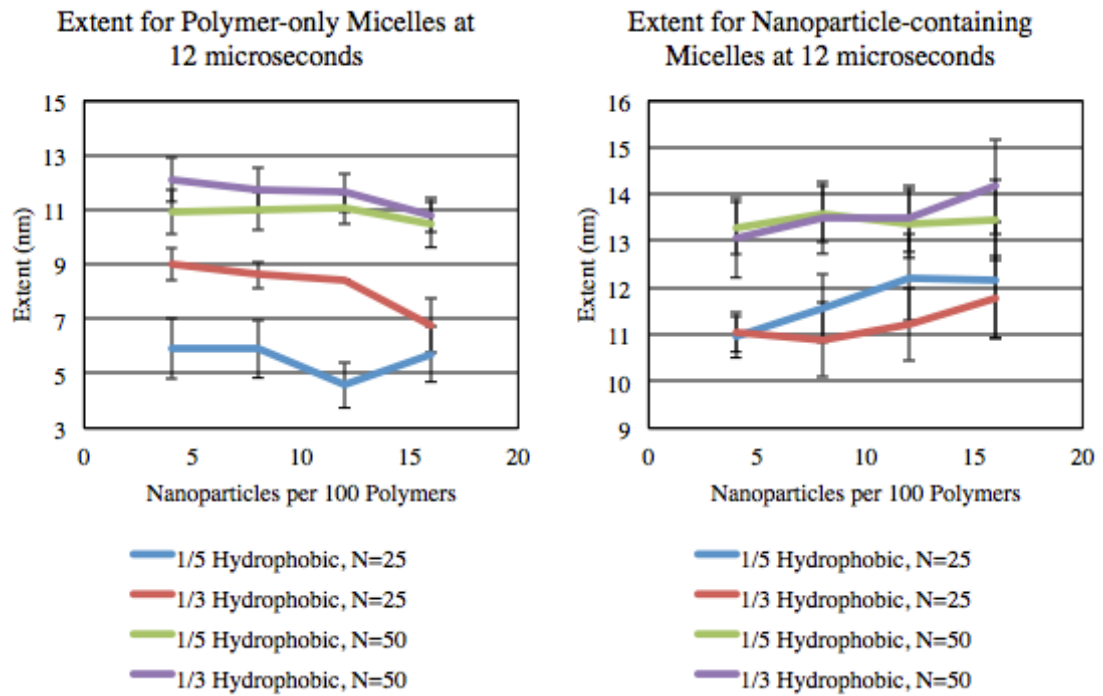


Figure 11: Average extent of micelles for all systems at time 12 microseconds

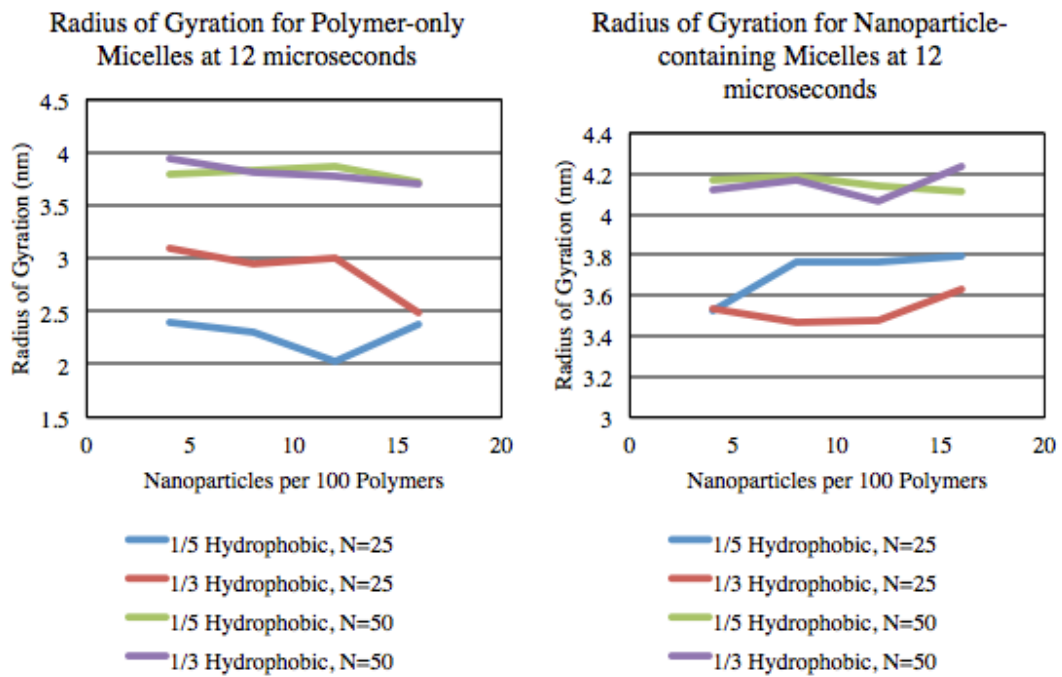


Figure 12: Radius of gyration of micelles for all systems at time 12 microseconds

Finally, to understand the amount of variation in these systems, the polydispersity of the number of beads was calculated by using the following equation:

$$\text{polydispersity} = 1 + \left(\frac{\text{Standard deviation of beads per micelle}}{\text{Mean of beads per micelle}} \right)^2.$$

This was calculated for polymer-only micelles and nanoparticle-containing micelles separately and is shown in Figure 13.

The polydispersity is relatively similar for all systems except it is significantly larger for the system with the smallest ratio of polymer hydrophobic beads per hydrophilic beads. This system is also the only system which continues to have free polymer at the end of the 12 microsecond simulation time; as discussed previously, the hydrophobic part may be able to be shielded by the relatively large hydrophilic part of

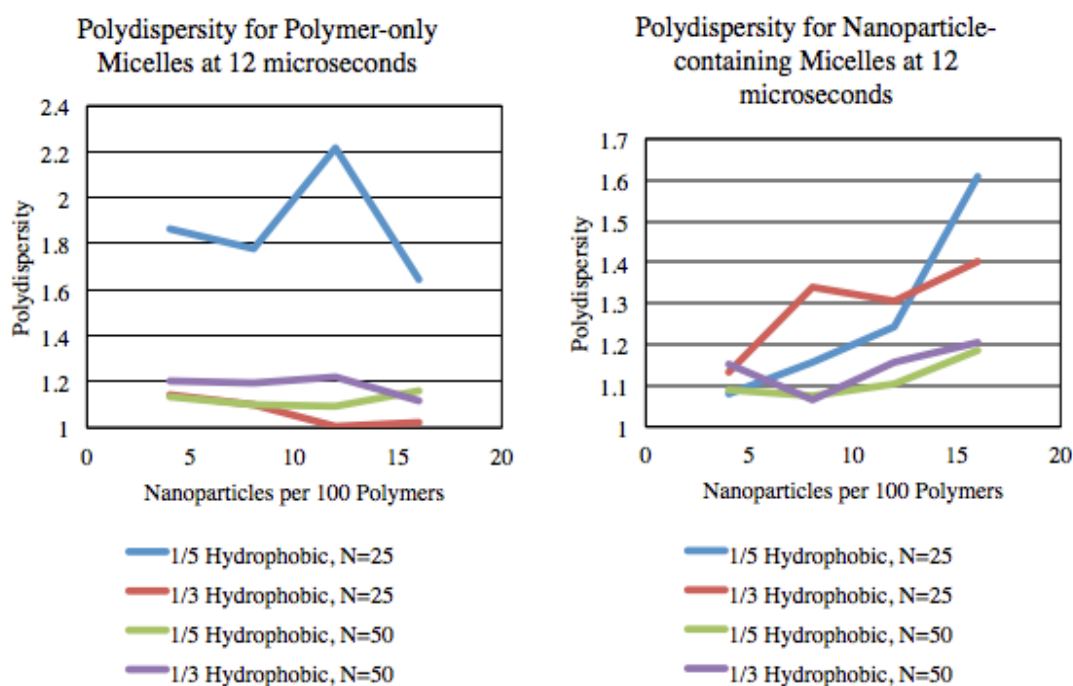


Figure 13: Polydispersity of micelles for all systems at time 12 microseconds

this polymer. The expectation is that this makes the free polymer relatively more stable and increases the barrier to nucleation of clusters. Generally, large micelles have a lower free energy than free polymers, but the free energy of a small cluster of polymers may be larger than that of the free polymers. Thus, there is a barrier to nucleation that means that small clusters will form only relatively rarely, and may break into free polymer again unless they grow well above the critical size beyond which increasing the size monotonically lowers the free energy. The driving force for nucleation of the clusters is the supersaturation (how much polymer is present versus the amount required to form stable micelles) (12). The free polymer is initially in equilibrium (does not prefer to form micelles in the good solvent), but quickly becomes supersaturated as the solvent is changed from good to poor. The amount of supersaturation initially increases with time due to the solvent change, but as micelles form the concentration of free polymer available to nucleate new micelles lowers, so the degree of supersaturation decreases. Thus, there is a finite time period during which nucleation typically occurs. Once a stable nucleus exists, it grows based on the concentration of free polymer available to be added (which decreases over time). The micelles that happened to nucleate early on will be more likely to grow to a larger size than those that nucleated later (causing polydispersity in micelle size). In this way, the nucleation barrier (how rare the nucleation event is and thus the spread in time over which the nuclei form) directly impacts the polydispersity of the system. Based on the current results, one could assume that the system which contains relatively stable free polymer has a higher nucleation barrier, leading to a larger

polydispersity, but this was not analyzed in detail. Other systems may participate in simple coagulation (clustering with no free energy barrier to nucleation) or nucleation on a faster timescale. A more detailed analysis of the free polymer and micelle size as a function of time, including very short times when micelle size is small and the micelles may occasionally break up, may lead to additional insights regarding which systems experience coagulation versus nucleation, and how the nucleation and growth processes impact the overall results, in future work. In addition, a more detailed analysis would reveal if the nanoparticle-containing micelles nucleate differently than the polymer-only micelles. Because there is a smaller degree of polydispersity for nanoparticle-containing micelles, these micelles may participate in simple coagulation; however, this would have to be studied more in depth to determine if this is the case.

Chapter 4: Conclusion

Polymer protection allows for the use of medical nanoparticles that are currently unable to be appropriately introduced into the body. In addition, hard nanoparticles can be used that could have magnetic or fluorescent properties, which allow them to be controlled with the use of magnetic fields and more easily imaged. However, current methods of polymer protecting medical nanoparticles have not reached their full commercial potential because the size and shape of the micelles created cannot be easily controlled. This project simulated the flash nanoprecipitation of micelles with hard nanoparticles and polystyrene-*b*-polyethylene glycol polymer. Results showed that longer polymers created a greater number of micelles, with a lower number of nanoparticles and polymers per micelle. In addition, some smaller micelles formed which contained only polymers; however, no nanoparticles were excluded from micelles. Almost all systems had no free polymer at the end of the simulations; however, those that did showed a greater polydispersity in polymer-only micelle size. These results can be used to control the size and composition of flash nanoprecipitated micelles.

In the future, larger systems should be studied for better statistical information. In addition, nanoparticles of varying sizes and compositions should be studied. Additionally, more in-depth data analysis can lead to an understanding of the mechanisms of micelle formation as a function of polymer length, concentration, and solvent strength. Knowing the mechanisms behind micelle formation can better inform

how to scale up the process to a commercial level with control of micelle size and polydispersity.

Chapter 5: References

1. Fraser, B., Denniston, C. and Muser, M. H. Diffusion, elasticity, and shear flow in self-assembled block copolymers: A molecular dynamics study. *Journal of Polymer Science Part B: Polymer Physics* **43**, 970–982 (2005).
2. Horsch, M. A., Zhang, Z., Iacovella, C. R. and Glotzer, S. C. Hydrodynamics and microphase ordering in block copolymers: Are hydrodynamics required for ordered phases with periodicity in more than one dimension? *The Journal of Chemical Physics* **121**, 11455–11462 (2004).
3. Hunenberger, P. Thermostat Algorithms for Molecular Dynamics Simulations. *Advanced Polymer Science* **173**, 105-149 (2005).
4. Soddemann, T., Dunweg, B., and Kremer, K. Dissipative particle dynamics: A useful thermostat for equilibrium and nonequilibrium molecular dynamics simulations. *Physical Review E* **68**, 046702(8) (2003).
5. Spaeth, J., Kevrekidis, I. and Panagiotopoulos, A. A comparison of implicit- and explicit-solvent simulations of self-assembly in block copolymer and solute systems. *The Journal of Chemical Physics* **134**, 164902(10) (2011).
6. Spaeth, J., Kevrekidis, I. and Panagiotopoulos, A. Dissipative particle dynamics simulations of polymer-protected nano particle self-assembly. *The Journal of Chemical Physics* **135**, 184903(10) (2011).

7. Pastorino, C., Kreer, T., Müller, M. and Binder, K. Comparison of dissipative particle dynamics and Langevin thermostats for out-of-equilibrium simulations of polymeric systems. *Physical Review E* **76**, 026706(10) (2007).
8. Wang, J., Weikun, L. and Zhu, J. Encapsulation of inorganic nanoparticles into block copolymer micellar aggregates: Strategies and precise localization of nanoparticles. *Polymer* **55** 1079-1096 (2014).
9. <http://compmech.lab.asu.edu/research.php>
10. Weinberg, Robert A. *The Biology of Cancer*. New York: Garland Science, 2007.
Print.
11. http://lammmps.sandia.gov/doc/pair_dpd.html
12. Johnson, B. and Prud'homme, R. Mechanism for Rapid Self-Assembly of Block Copolymer Nanoparticles. *Physical Review Letters* **91(11)**, 118302(4) (2003).

Appendix A: Data

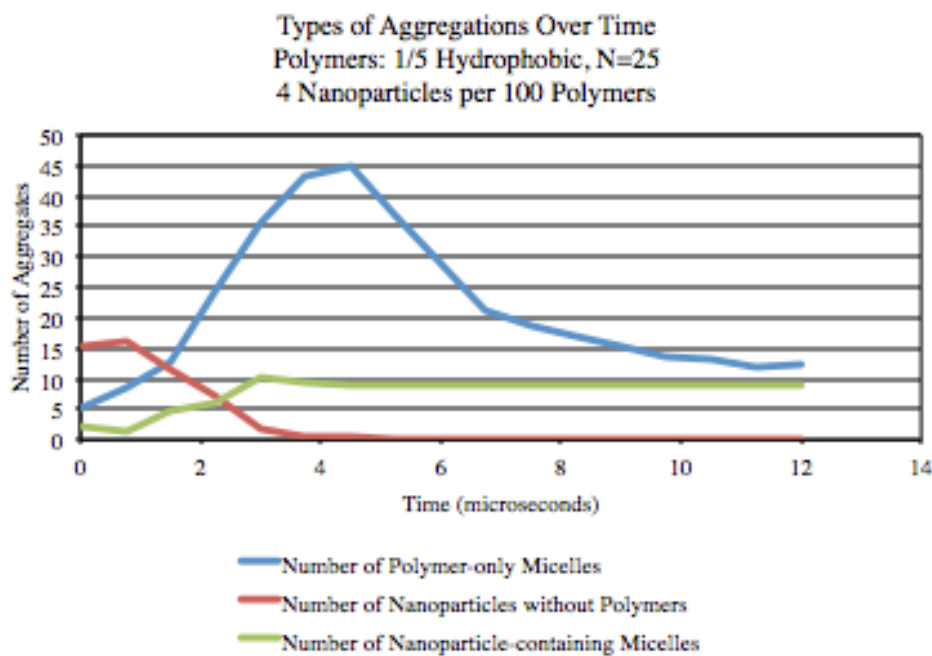
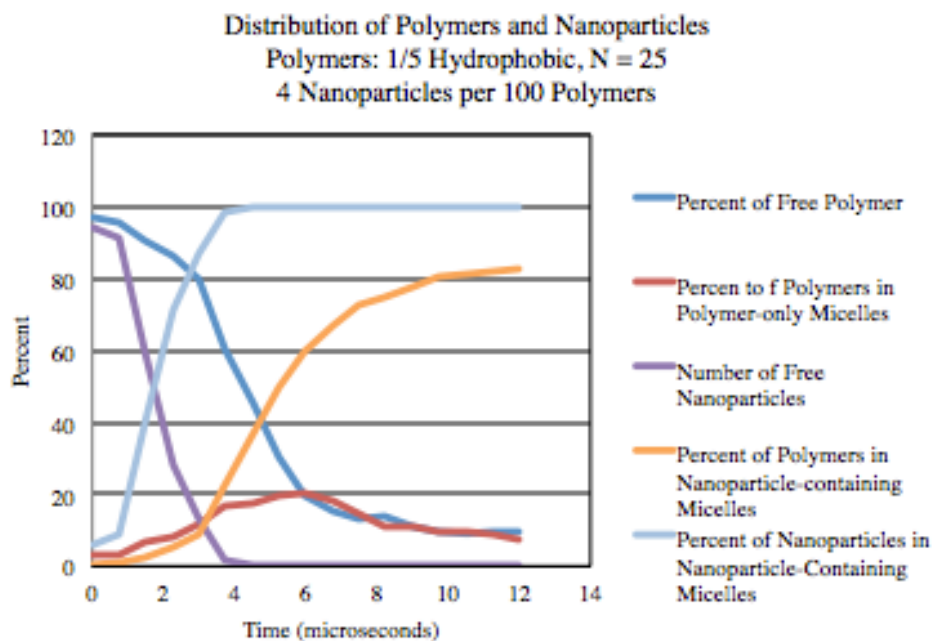
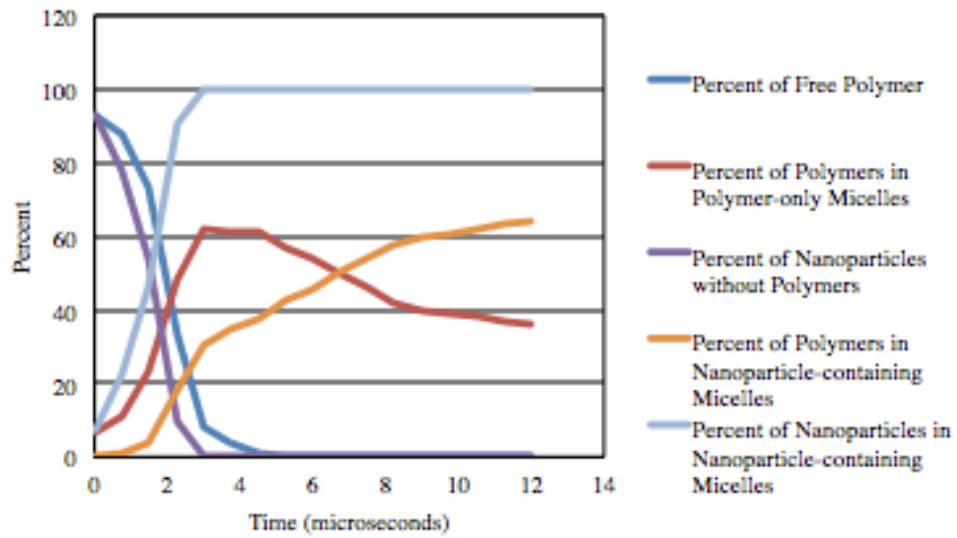


Figure 14

Distribution of Polymers and Nanoparticles
 Polymers: 1/3 Hydrophobic, N = 50
 4 Nanoparticles per 100 Polymers



Types of Aggregations Over Time
 Polymers: 1/3 Hydrophobic, N=50
 4 Nanoparticles per 100 Polymers

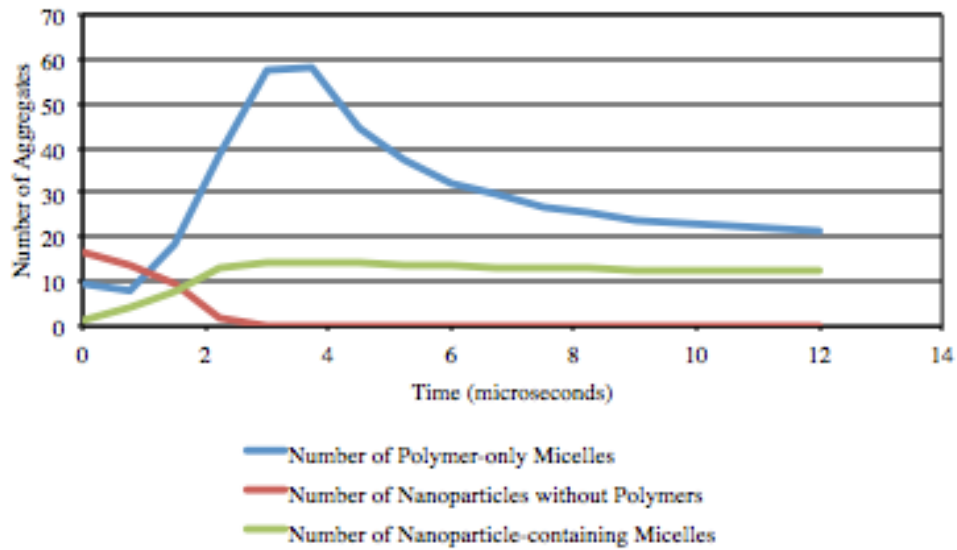
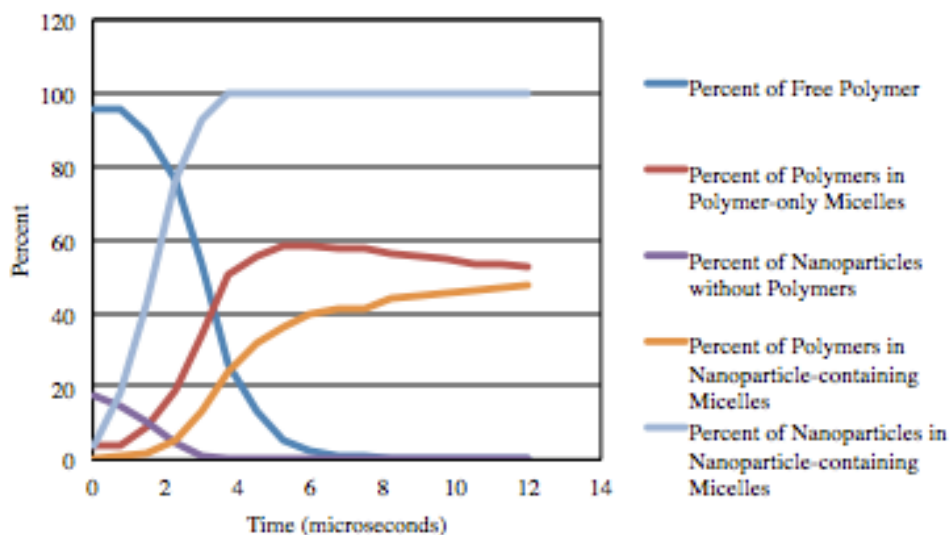


Figure 15

Distribution of Polymers and Nanoparticles
 Polymers: 1/5 Hydrophobic, N = 50
 4 Nanoparticles per 100 Polymers



Types of Aggregations Over Time
 Polymers: 1/5 Hydrophobic, N=50
 4 Nanoparticles per 100 Polymers

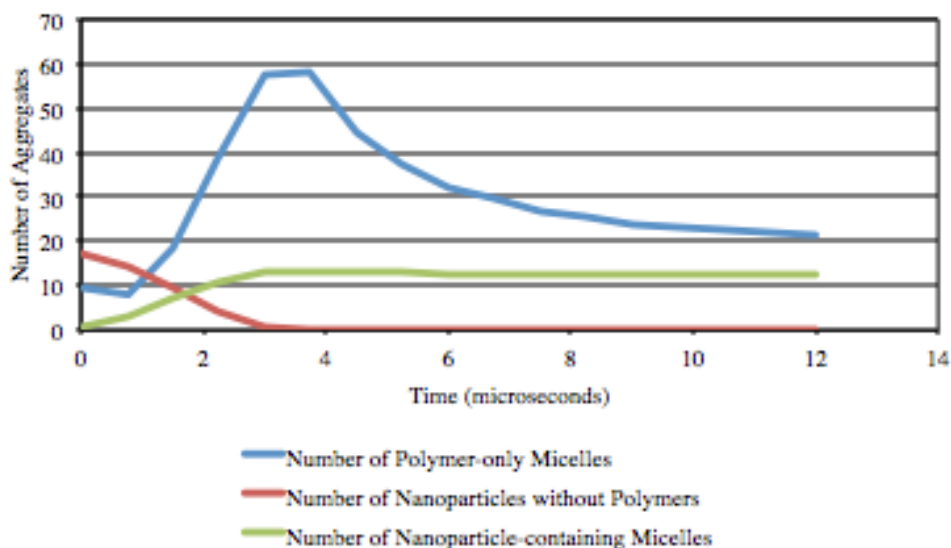
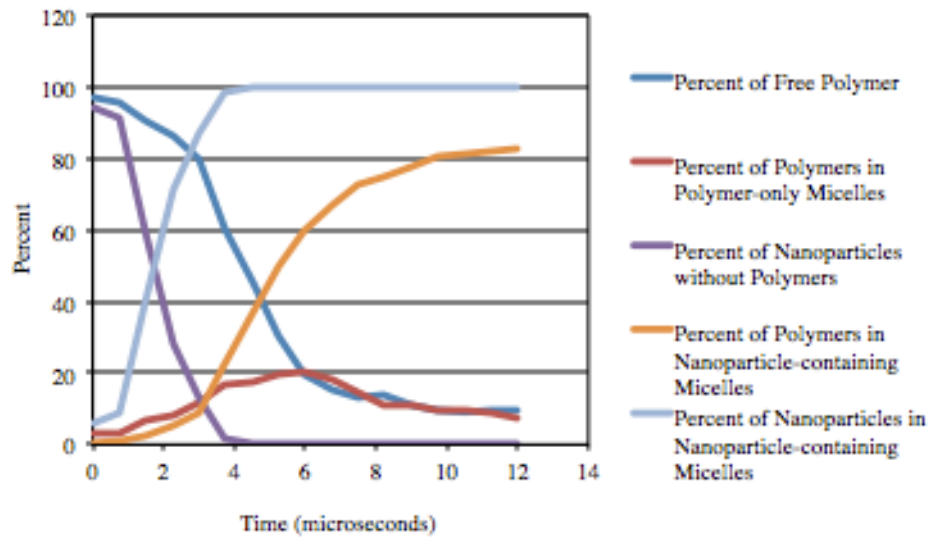


Figure 16

Distribution of Polymers and Nanoparticles
 Polymers: 1/5 Hydrophobic, N = 25
 8 Nanoparticles per 100 Polymers



Types of Aggregations Over Time
 Polymers: 1/5 Hydrophobic, N=25
 8 Nanoparticles per 100 Polymers

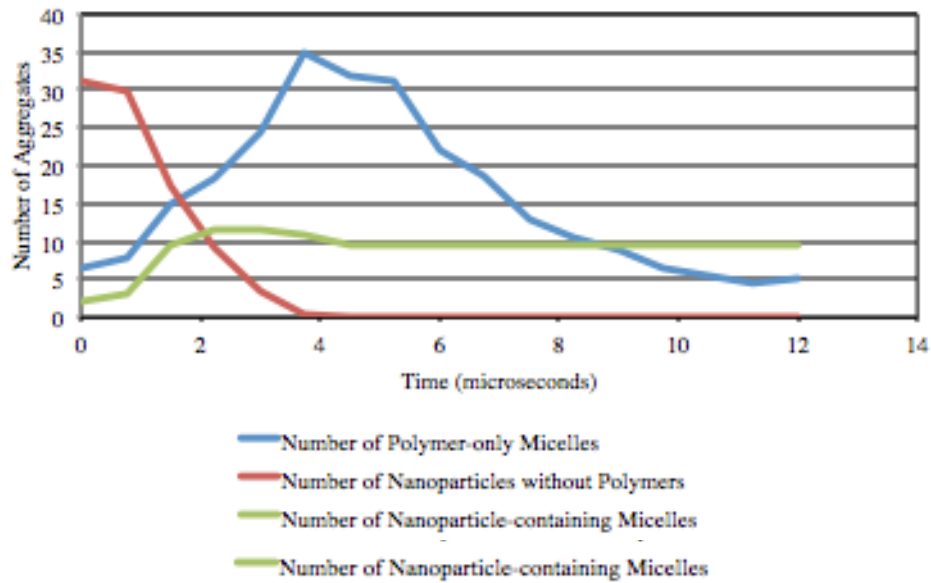
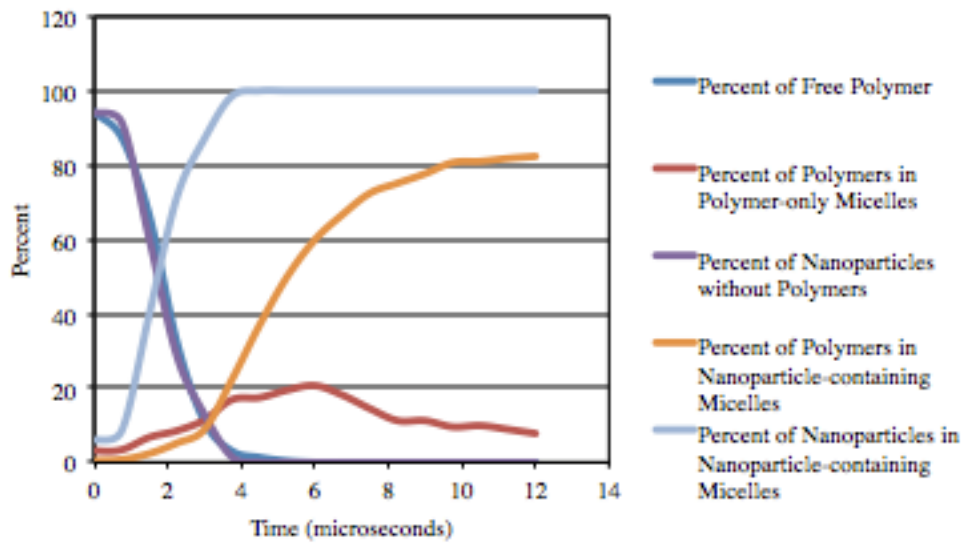


Figure 17

Distribution of Polymers and Nanoparticles
 Polymers: 1/3 Hydrophobic, N = 50
 8 Nanoparticles per 100 Polymers



Types of Aggregations Over Time
 Polymers: 1/3 Hydrophobic, N = 50
 8 Nanoparticles per 100 Polymers

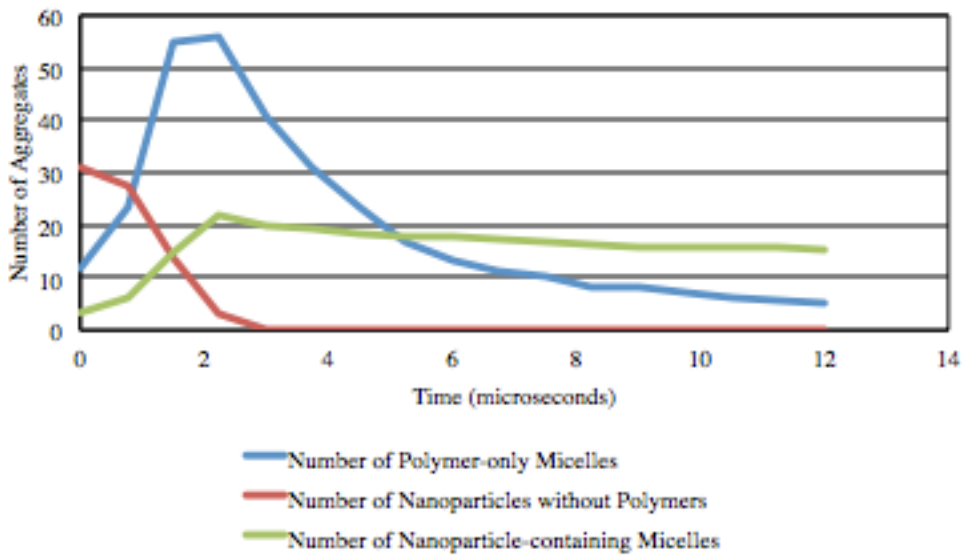
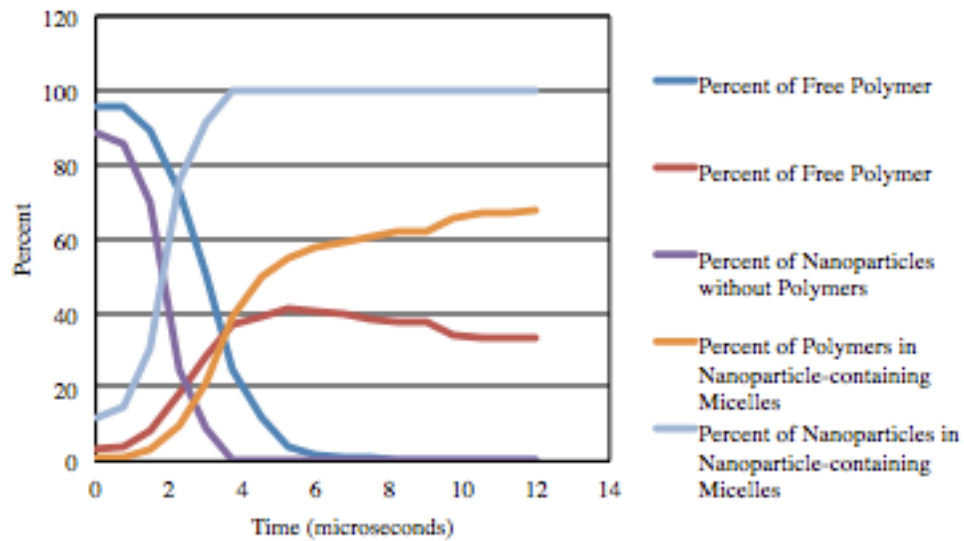


Figure 18

Distribution of Polymers and Nanoparticles
 Polymers: 1/5 Hydrophobic, N = 50
 8 Nanoparticles per 100 Polymers



Types of Aggregations Over Time
 Polymers: 1/5 Hydrophobic, N=50
 8 Nanoparticles per 100 Polymers

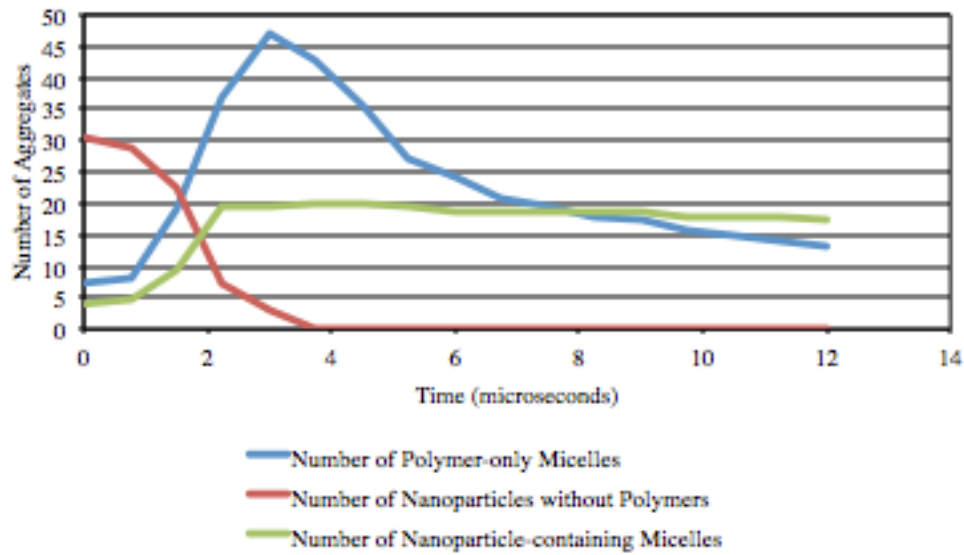
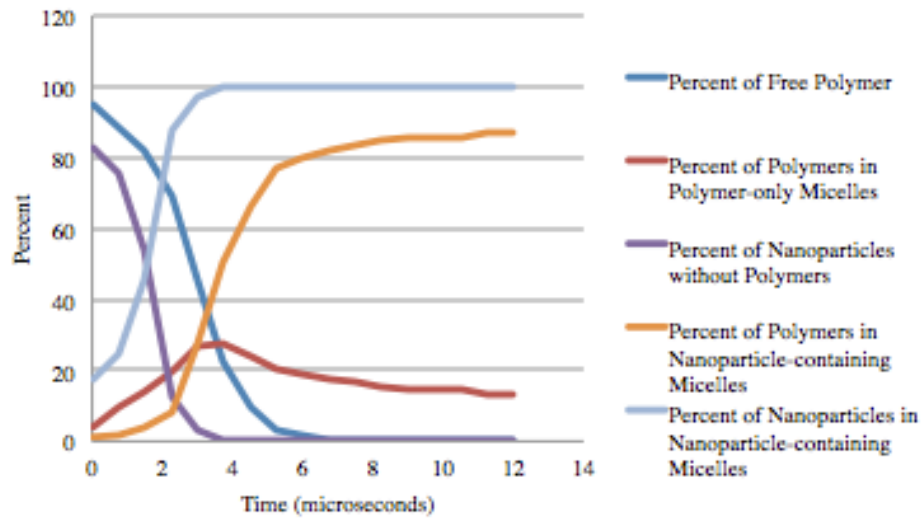


Figure 19

Distribution of Polymers and Nanoparticles
 Polymers: 1/3 Hydrophobic, N = 25
 8 Nanoparticles per 100 Polymers



Types of Aggregations Over Time
 Polymers: 1/3 Hydrophobic, N=25
 8 Nanoparticles per 100 Polymers

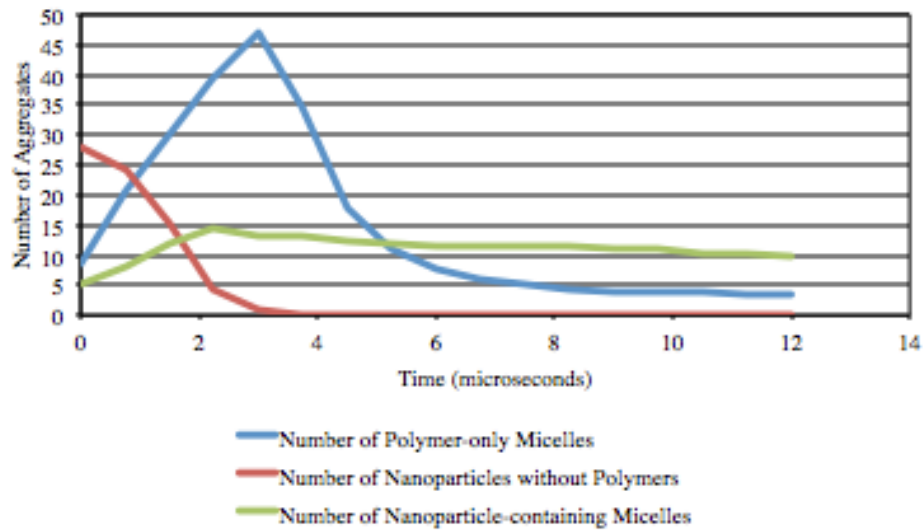
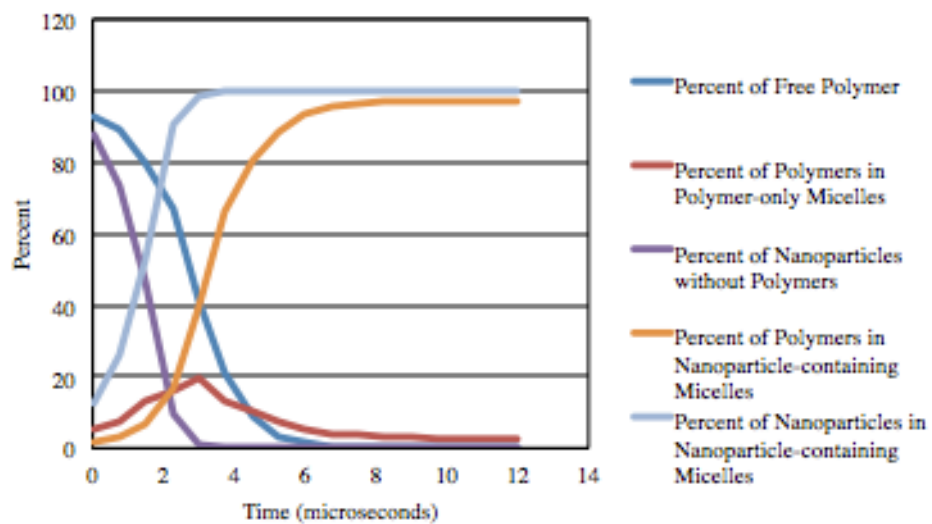


Figure 20

Distribution of Polymers and Nanoparticles
 Polymers: 1/3 Hydrophobic, N = 25
 12 Nanoparticles per 100 Polymers



Types of Aggregations Over Time
 Polymers: 1/3 Hydrophobic, N=25
 12 Nanoparticles per 100 Polymers

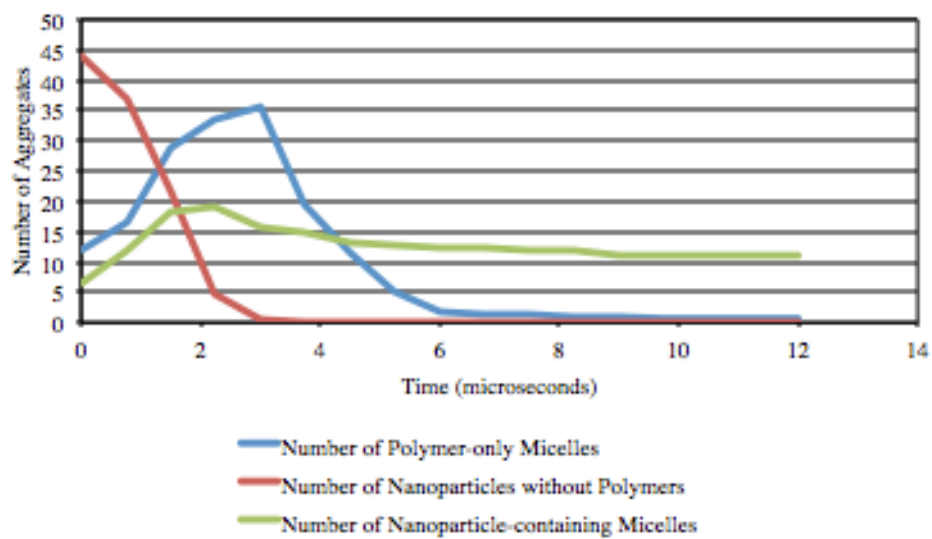
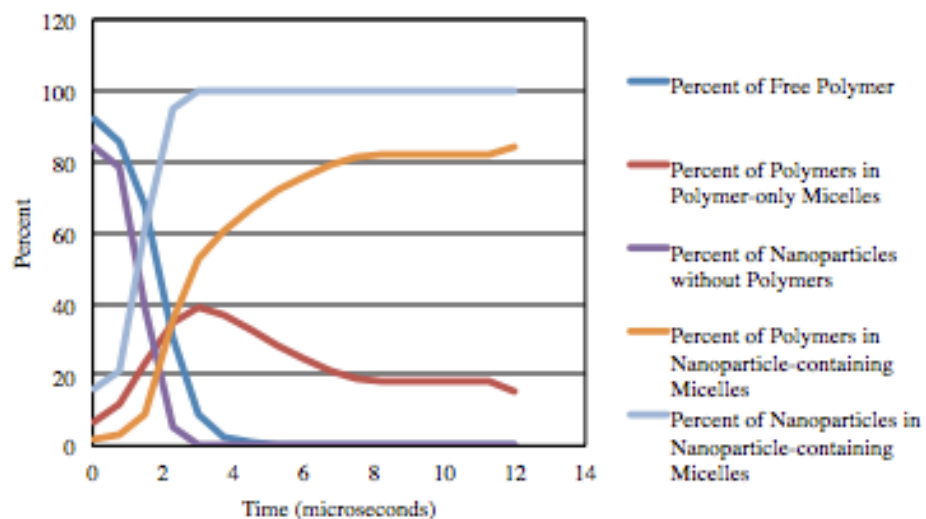


Figure 21

Distribution of Polymers and Nanoparticles
 Polymers: 1/3 Hydrophobic, N = 50
 12 Nanoparticles per 100 Polymers



Types of Aggregations Over Time
 Polymers: 1/3 Hydrophobic, N=50
 12 Nanoparticles per 100 Polymers

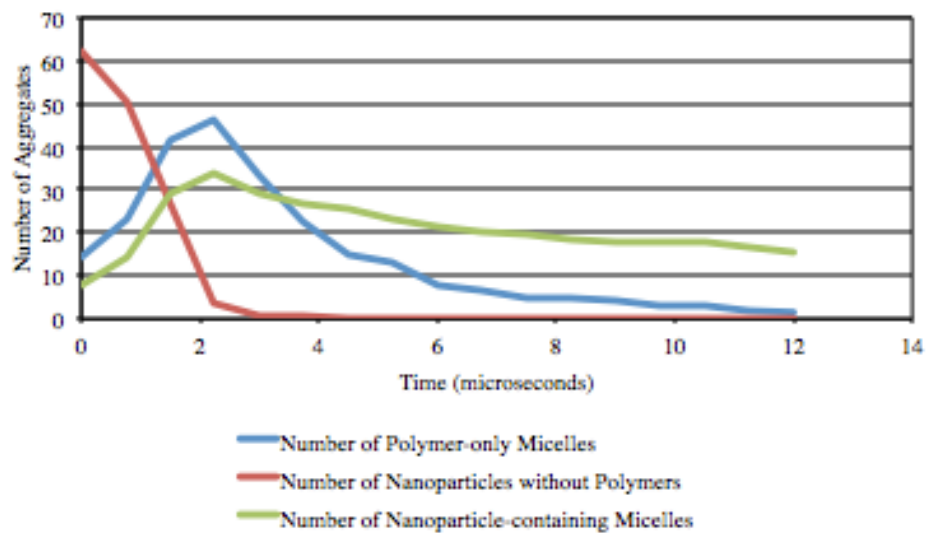
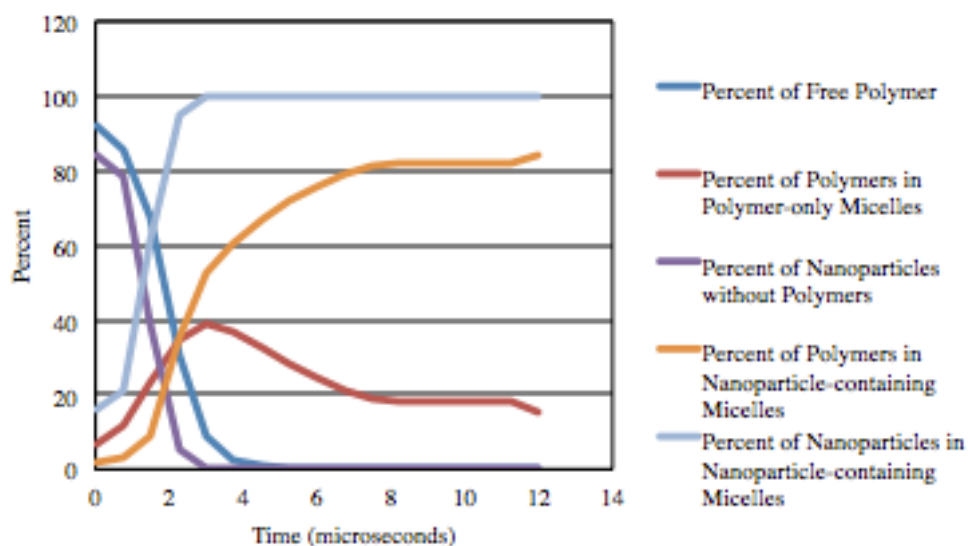


Figure 22

Distribution of Polymers and Nanoparticles
 Polymers: 1/3 Hydrophobic, N = 50
 12 Nanoparticles per 100 Polymers



Types of Aggregations Over Time
 Polymers: 1/3 Hydrophobic, N=50
 12 Nanoparticles per 100 Polymers

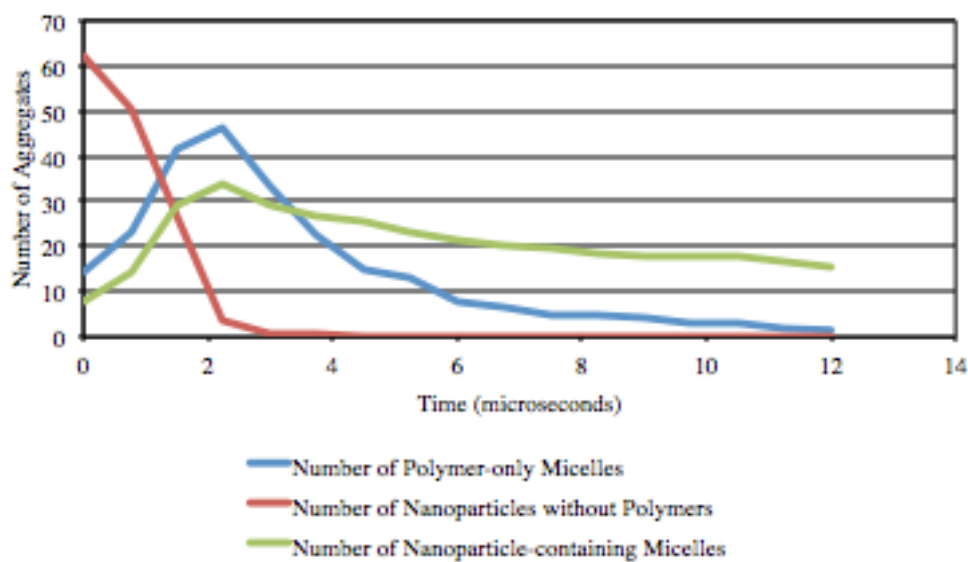
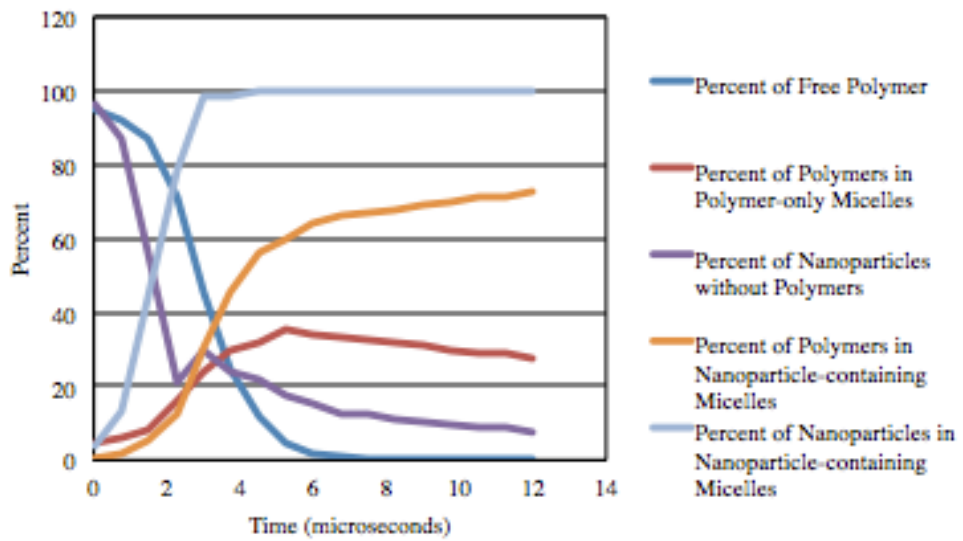


Figure 23

Distribution of Polymers and Nanoparticles
 Polymers: 1/5 Hydrophobic, N = 50
 12 Nanoparticles per 100 Polymers



Types of Aggregations Over Time
 Polymers: 1/5 Hydrophobic, N=50
 12 Nanoparticles per 100 Polymers

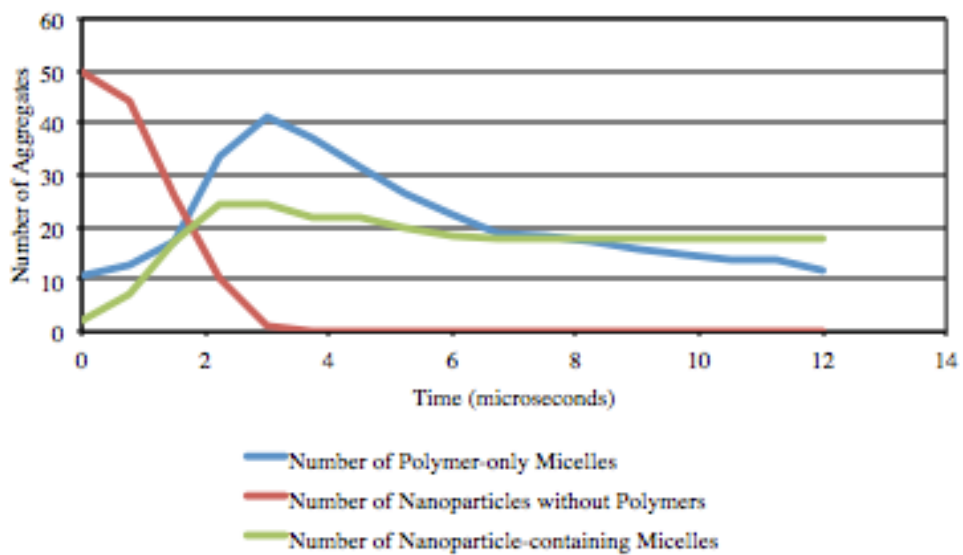


Figure 24

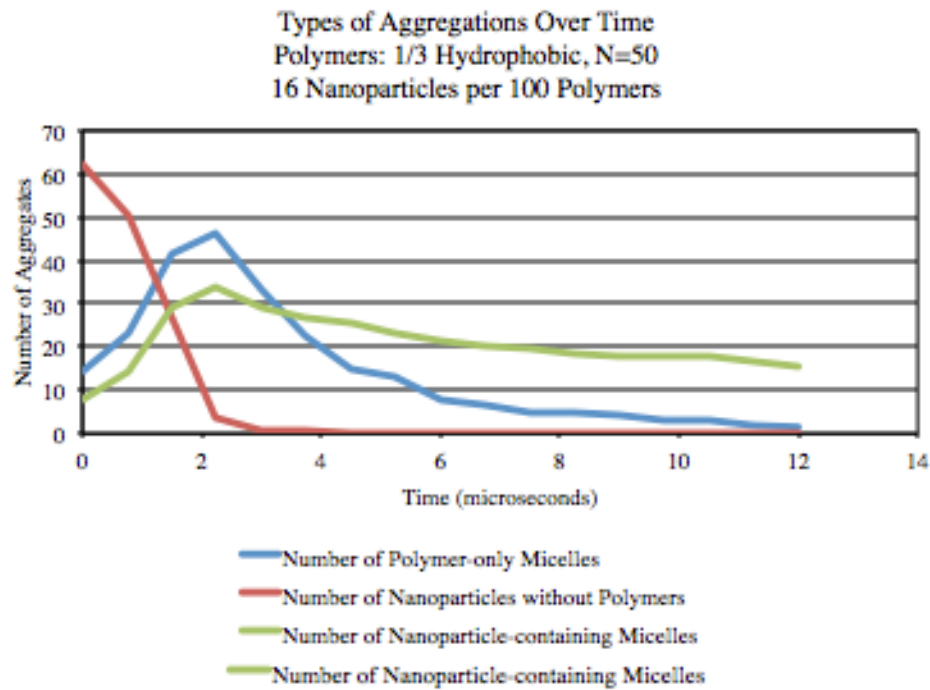
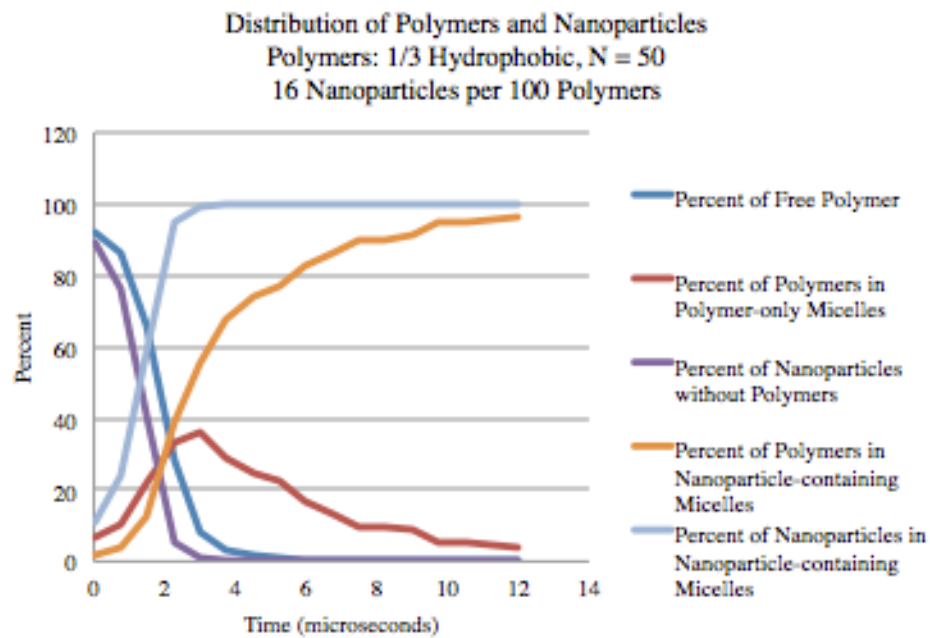
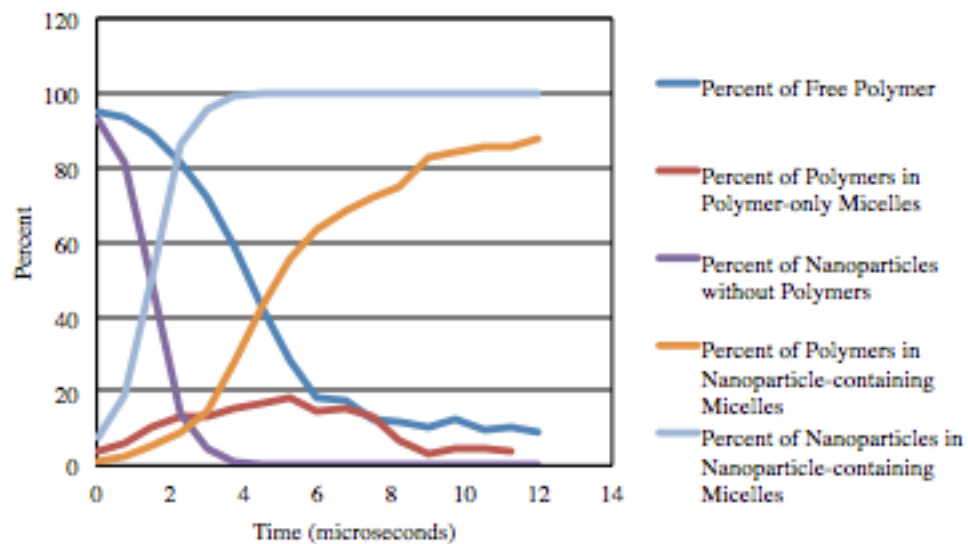


Figure 25

Distribution of Polymers and Nanoparticles
 Polymers: 1/5 Hydrophobic, N = 25
 16 Nanoparticles per 100 Polymers



Types of Aggregations Over Time
 Polymers: 1/5 Hydrophobic, N=25
 16 Nanoparticles per 100 Polymers

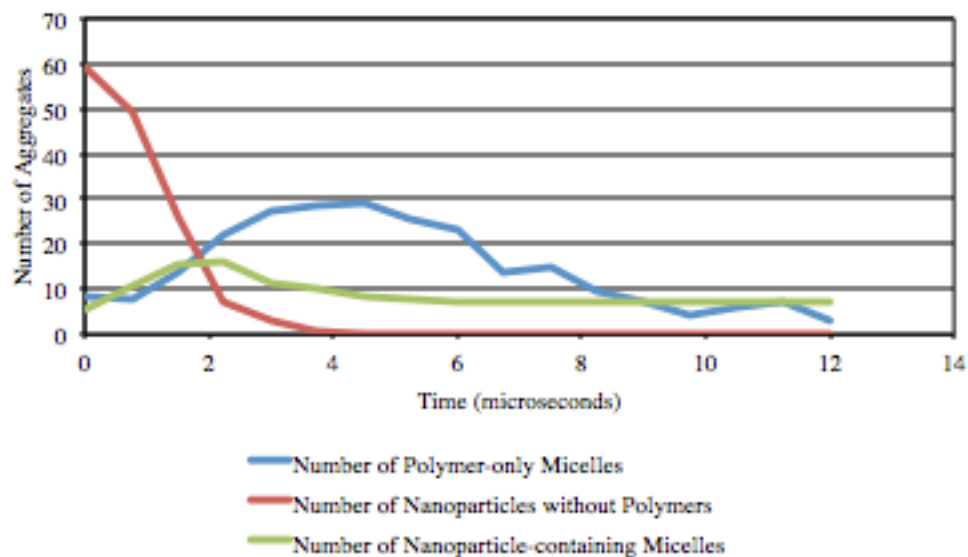


Figure 26

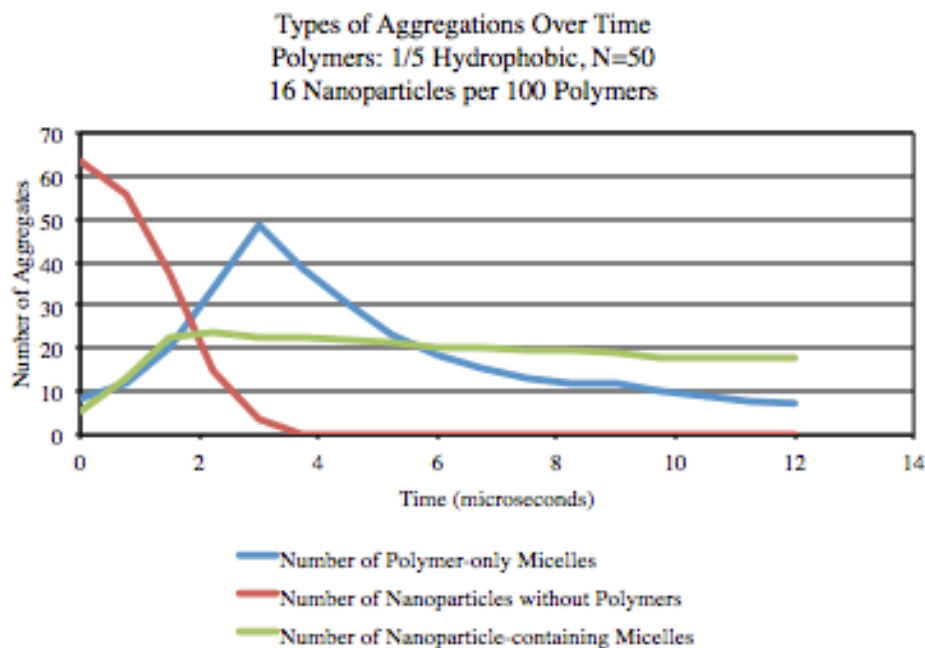
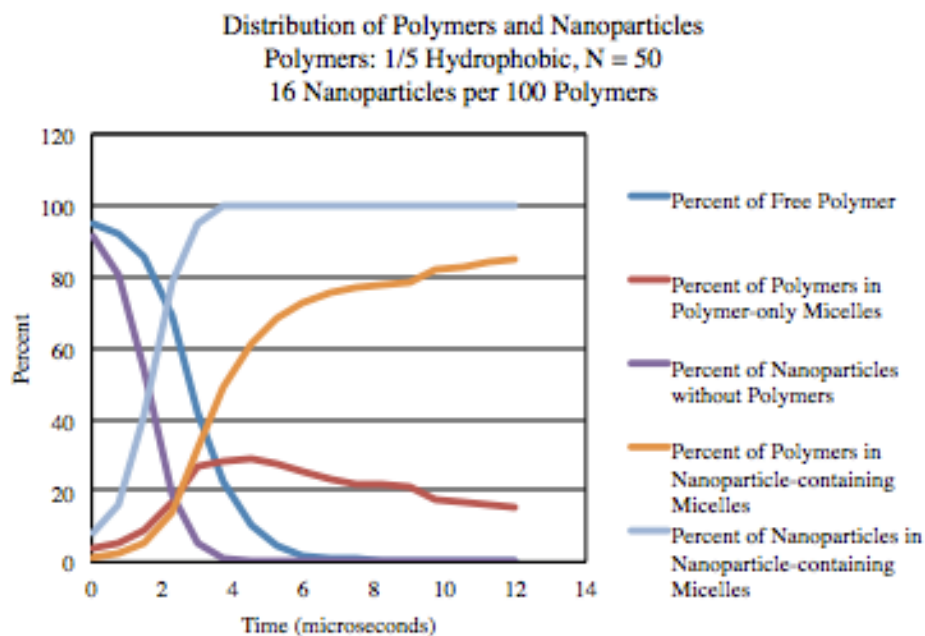


Figure 27

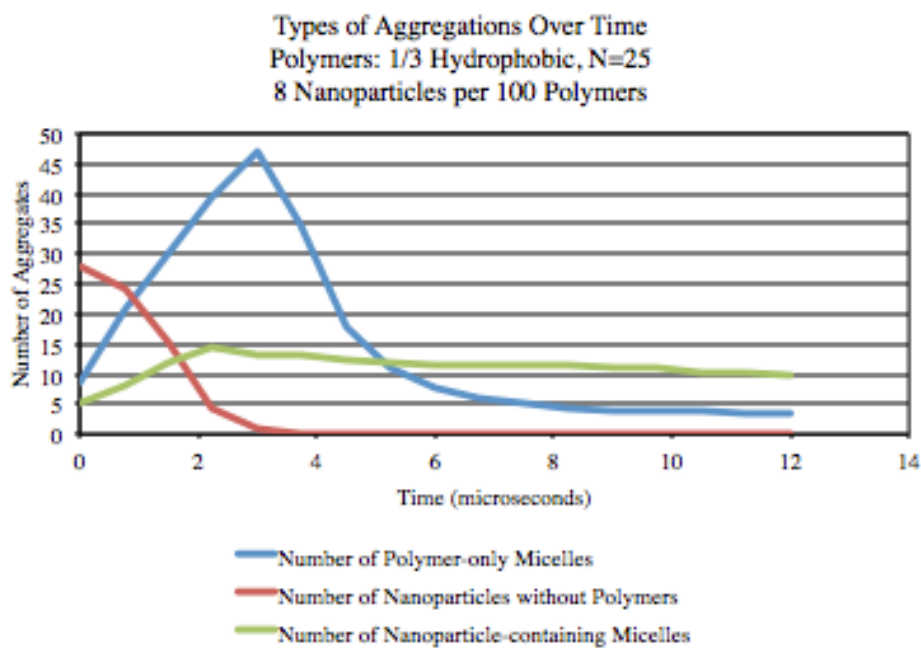
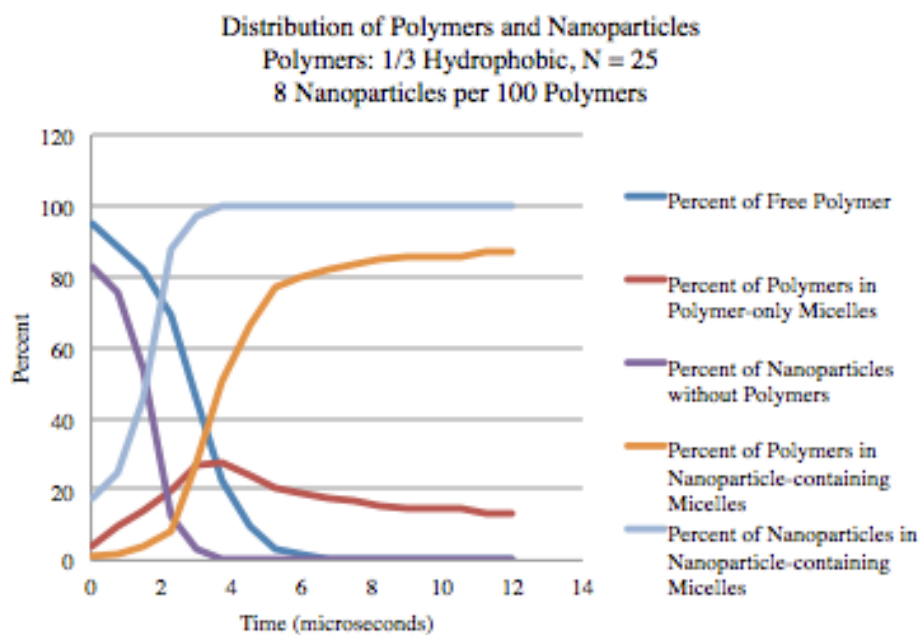
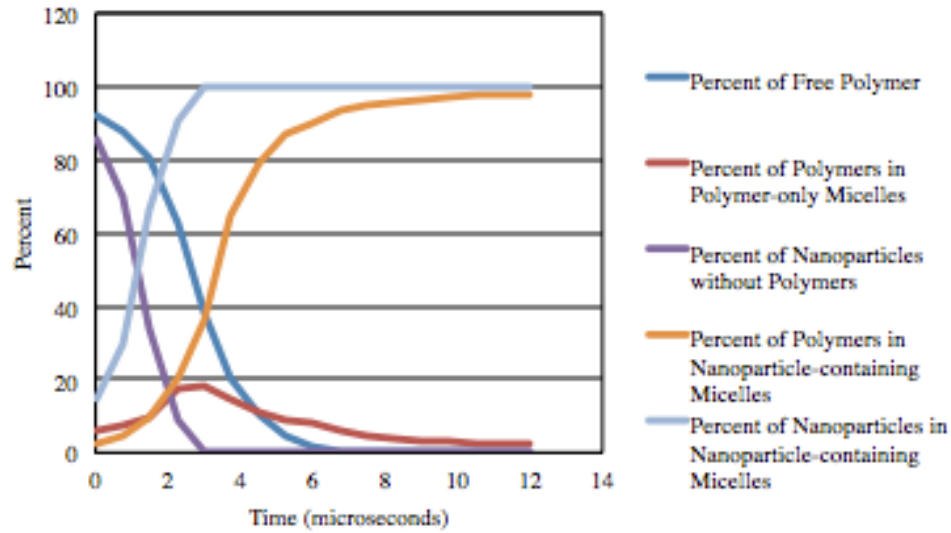


Figure 28

Distribution of Polymers and Nanoparticles
 Polymers: 1/3 Hydrophobic, N = 25
 16 Nanoparticles per 100 Polymers



Types of Aggregations Over Time
 Polymers: 1/3 Hydrophobic, N=25
 16 Nanoparticles per 100 Polymers

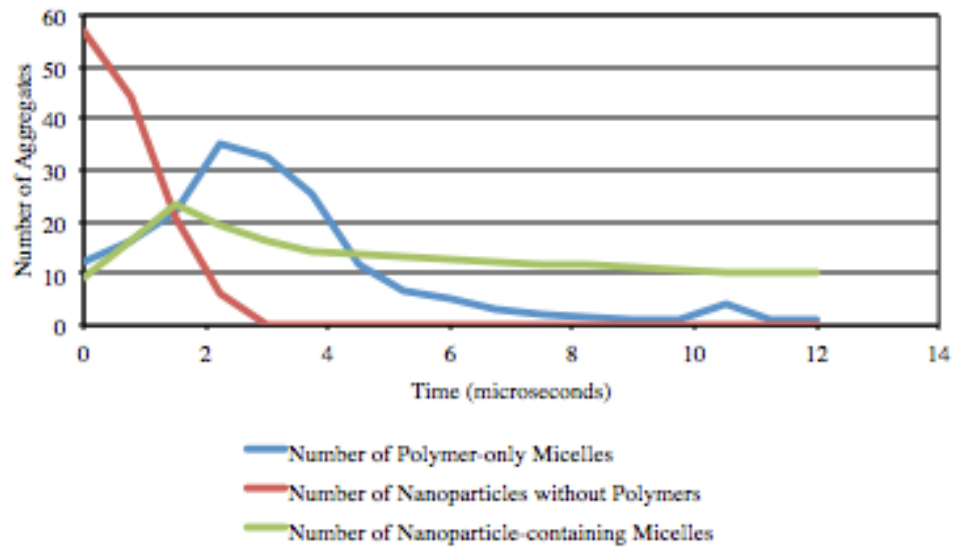


Figure 29